A bulk model for separation in hydrocyclones

A. B. Holland-Batt B.Sc., Ph.D., D.I.C., A.R.S.M., C.Eng., M.I.M.M.
Mineral Deposits, Ltd., Southport, Queensland, Australia

53.072:622.755.7

Synopsis
The performance of a hydrocyclone has been analysed in terms of bulk flow behaviour and average retention times. The conventional practice of determining the cut size by equating the radial velocities of the outward particle motion and the inward suspension flow has been replaced by solving the simplified continuity equation for the particle flux to determine the absolute particle velocity relative to the cyclone wall. The radial suspension flow is then introduced to determine the relative velocity between particle and fluid from which the d_{50} size is calculated. Expressions for the d_{50} size are developed for both spherical and irregular shaped particles and the effect of the volume concentration of particles in the feed is considered.

The published literature that relates to hydrocyclones provides comprehensive descriptions of investigations into virtually every aspect of hydrocyclone performance, ranging from fundamental studies of fluid flow and single-particle behaviour to empirically based models designed for use in control applications. Much of the fundamental work has been devoted to analysing what might be termed the microstructure of fluid and particle behaviour in the hope of obtaining time-variant or dynamic performance models. The evident complexity of this microstructure has provided a fruitful field for research, but only a limited consensus in the findings.

In the present paper attention is concentrated on the macro-structure with the object of deriving a simple model based on bulk flow considerations and incorporating the minimum number of variables necessary to provide realistic predictions of separation sizes. The approach adopted is to determine the retention time and extent of tangential motion for the suspension, then to develop the necessary relationship between particle velocities and volume concentrations by solving the continuity equation for the particle fluxes and, finally, to relate the radial velocity of the particles back to the corresponding particle size.

The analysis that follows assumes optimal separation conditions and is developed, initially, for low volume concentrations of particles in the feed suspension so that concentration effects do not interfere with the relative motion between particles and fluid. Corrections for higher concentrations are considered subsequently.

Separation at low solids concentrations

The analysis of the separation falls naturally into three stages: calculation of the bulk retention time and angular motion, the solution of the continuity equation to find the radial particle velocity and determination of the particle size that corresponds to the radial velocity.

Bulk retention time

The average tangential velocity (v) of the suspension entering the cyclone is determined by the pressure drop across the cyclone.* Expressed in terms of the total fluid head (h), this may be calculated as[1]

$$v = \sqrt{2gh} \tag{1}$$

Based on this velocity and the diameter (D) of the hydrocyclone, the acceleration (a) generated is

$$a = \frac{2v^2}{D} = \frac{4gh}{D} \tag{2}$$

To determine the bulk retention time (t), the internal volume (V_c) of the cyclone and the volumetric flow rate (Q) through the cyclone must be known. For a cyclone with the dimensions shown in Fig. 1 V_c can be estimated as

$$V_c = \frac{\pi D^3}{4}\left(n_1 + \frac{n_2}{3}\right) \tag{3}$$

Hence the average or bulk retention time is given by

$$t = \frac{V_c}{Q} \tag{4}$$

and in time t the suspension will have travelled a distance vt, which can be converted to the equivalent angular motion by dividing by the radius of motion ($D/2$):

$$\alpha = \frac{2vt}{D} \tag{5}$$

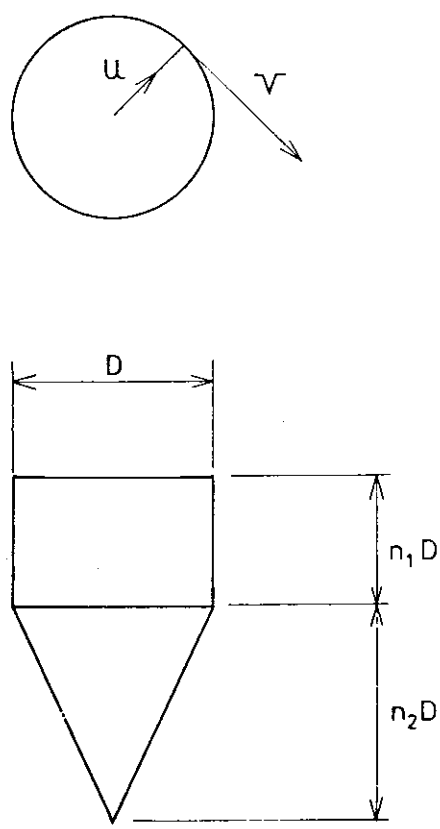

Fig. 1 Hydrocyclone parameters

*Definitions of the symbols used in this paper are given on page C25.

Manuscript first received by the Institution of Mining and Metallurgy on 24 August, 1981; revised manuscript received on 14 December, 1981. Paper published in *Trans. Instn Min. Metall. (Sect. C: Mineral Process Extr. Metall.)*, **91**, March 1982.

Continuity equation

The continuity equation for the flux of particles within the cyclone defines the relationship between the volume concentration (C_v) of solids in the suspension, the particle velocities (u, v) in the radial and tangential directions (see Fig. 1) and the extent of angular motion (α).

The particle fluxes (E_r, E_α) in the radial and tangential directions are defined as

$$E_r = uC_v \tag{6}$$

$$E_\alpha = vC_v \tag{7}$$

In terms of these quantities the general continuity equation for two-dimensional flow[2] becomes

$$\frac{\partial (rE_r)}{\partial r} + \frac{\partial E_\alpha}{\partial \alpha} = 0 \tag{8}$$

The use of average or bulk parameters simplifies the analysis considerably because u and v are considered to be constant and C_v becomes a function only of α. Equations 6, 7 and 8 may be combined and simplified to give

$$uC_v + v\frac{dC_v}{d\alpha} = 0 \tag{9}$$

If the volume concentration of particles of a given size entering the cyclone is C_{v0} and this value falls to a level C_v by the time the depleted suspension has traversed α radians of motion and exits via the overflow, on integrating equation 9 between these limits

$$u = \frac{v}{\alpha} \ln \left(\frac{C_{v0}}{C_v}\right) \tag{10}$$

The radial velocity u is the net value relative to the frame of reference, i.e. the walls of the cyclone. It is, in fact, the resultant of two components – the particle velocity (u_p) relative to the fluid and the opposing radial fluid velocity (U) resulting from the migration of the fluid from the periphery of the cyclone to the central axis. The average value of U may be estimated from the volume flow Q and the wall area (A_c) parallel to the central axis (see Fig. 1):

$$A_c = \pi D^2\left(n_1 + \frac{n_2}{2}\right) \tag{11}$$

$$U = \frac{Q}{A_c} \tag{12}$$

Thus, the particle velocity relative to the fluid is given by

$$u_p = U + \frac{v}{\alpha} \ln \left(\frac{C_{v0}}{C_v}\right) \tag{13}$$

If equations 3, 4, 5, 11, 12 and 13 are combined, the expression for u_p can be rearranged to give

$$u_p = \frac{Q}{A_c} + \frac{QD}{2V_c} \ln \left(\frac{C_{v0}}{C_v}\right) \tag{14}$$

Velocity–size correlation

Particle motion relative to a fluid is governed by two opposing forces – the body force generated by the applied acceleration and the drag force exerted by the fluid on the particle. If the forces are in equilibrium, a terminal velocity (u_T) is attained and the drag coefficient (C_T) takes a corresponding terminal value

$$V_p(\sigma - \rho)a = \tfrac{1}{2}\rho u_T^2 A_x C_T \tag{15}$$

The particle volume (V_p) is a function of particle size and can be calculated directly for regular geometric shapes. Some form of shape coefficient is required to deal with the irregular shaped particles more commonly encountered, and in the present instance the system devised by Heywood[3] is employed. This defines a volume coefficient (k) such that the volume of the particle is related to the equivalent projected area diameter (d) as follows:

$$V_p = kd^3 \tag{16}$$

On combining equations 15 and 16, the relationship between d and u_T for spherical particles ($k = \pi/6$) may be written as

$$d = \frac{3C_T}{4} \frac{\rho u_T^2}{(\sigma - \rho)a} \tag{17}$$

The drag coefficient, C_T, is a function of the Reynolds number (R_T) and the volume coefficient, k, and the form of this relationship must be established before equation 17 can be used to calculate d. The tabular methods developed by Heywood[3] can be employed, but with a slight reduction in accuracy an equation can be derived that gives a more convenient solution.

It is generally assumed[4] that the radial motion of particles in a hydrocyclone falls in the laminar regime, and under these conditions a simplified analysis is possible. C_T is then simply related to the Reynolds numbers:

$$C_T = \frac{E}{R_T} \tag{18}$$

where

$$R_T = \frac{u_T d\rho}{\eta} \tag{19}$$

Combining equations 17, 18 and 19 gives the relationship between particle size and velocity under laminar conditions:

$$d = \sqrt{\frac{3E}{4} \frac{\eta u_T}{(\sigma - \rho)a}} \tag{20}$$

Table 1 Values of coefficient E

Volume coefficient, k	Coefficient E From tables[3]	From equation 21
0.1	94	96
0.2	59	60
0.3	42	42
0.4	33	33
Spheres $\pi/6$	24	–

From the data in Heywood's tables[3] values of E were derived for the various shape groups denoted by volume coefficients ranging from 0.1 to 0.4. The results are given in the second column of Table 1, and in the third column the values given by the approximation equation

$$E = 24\left(1 + \frac{6}{2^{10k}}\right) \tag{21}$$

which, on substitution in equation 18, gives

$$C_T = \frac{24}{R_T}\left(1 + \frac{6}{2^{10k}}\right) \quad (22)$$

The performance model can now be summarized and put into appropriate form: for the average cut size (d_{50}) the ratio C_v/C_{v0} takes the value 0.5, so on inserting this in equation 14 and substituting u_p for u_T in equation 20, equations 14, 20 and 21 may be rewritten:

$$u_p = \frac{Q}{A_c} + \frac{QD}{2V_c} \ln(2) \quad (23)$$

$$d_{50} = \sqrt{18\left(1 + \frac{6}{2^{10k}}\right)\frac{\eta u_p}{(\sigma - \rho)a}} \quad (24)$$

The model has been tested against the average performance data quoted by a hydrocyclone manufacturer[5] for sand particles (sp.gr. 2.65) in water. The data have been reproduced in Table 2 together with the estimated internal areas and volumes of the hydrocyclones. The d_{50} sizes predicted by equations 23 and 24 with a volume coefficient of 0.3 are given in Table 3 and have been plotted in Fig. 2 along with the ranges quoted in Table 2.

The calculated d_{50} sizes are about 1 μm low for cyclones of diameter 10—20 mm, but thereafter are within the manufacturer's range for cyclones up to 500 mm in diameter. The predictions for 750 mm and 1200 mm are high by roughly 10 and 20 μm, respectively. There are a number of possible explanations for this discrepancy, but the most likely cause is incorrect estimation of some of the factors that contribute to the average retention time.

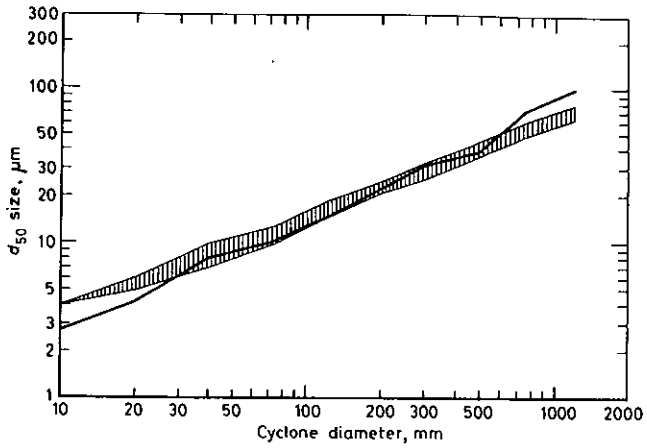

Fig. 2 d_{50} predictions (0% solids)

The validity of assuming laminar motion has been checked by calculating the Reynolds numbers for the particle-fluid motion and the results are included in Table 3. Taking an upper limit of 1 for laminar motion, cyclones of diameter 200 mm and upwards experience separation conditions that fall in the lower part of the transitional regime, but the error introduced is not large and is probably an acceptable price to pay for simplicity of calculation.

Effect of volume concentration

Increasing volume concentrations of particles affect the separation in two different ways. The primary effect is an interaction between neighbouring particles, which arises from hydrodynamic considerations and tends to reduce the particle velocities and increase the separation sizes. The

Table 2 AKA vortex hydrocyclone data

Cyclone diameter, mm	Pressure drop, bar	Capacity, m³/h	Area, cm²	Volume, cm³	Separation size ranges, μm Low concentration From	To	250 g/l From	To
10	4	0.3	32	8	4	4	—	—
20	3	0.7	90	43	5	6	—	—
40	2	2	215	185	7	10	—	—
75	2	7	825	1 370	10	13	20	25
125	1.5	18	2 205	6 150	15	19	30	38
200	1	32	4 260	18 100	21	25	40	50
300	1	75	7 720	48 490	26	33	50	65
500	0.7	134	20 825	219 600	37	46	75	92
750	0.5	260	26 915	405 560	50	62	100	125
1200	0.3	390	55 755	1 368 930	65	80	130	160

Table 3 Predicted separation (σ = 2.65, k = 0.3)

Cyclone diameter, mm	Tangential velocity, cm/s	Radial acceleration, g	Total angle, rad	Radial velocity, cm/s	d_{50}, μm	Reynolds number
10	2829	16 315	533.2	6.33	2.8	0.17
20	2450	6 118	538.3	5.43	4.2	0.23
40	2000	2 039	335.4	6.73	8.0	0.54
75	2000	1 088	376.0	6.06	10.4	0.63
125	1732	489	341.0	5.80	15.2	0.88
200	1414	204	287.9	5.50	22.9	1.26
300	1414	136	219.5	7.19	32.1	2.31
500	1183	57	279.2	4.74	40.2	1.91
750	1000	27	149.3	7.41	72.8	5.39
1200	775	10	162.8	5.34	101.0	5.40

secondary effect comes into operation when the solids handling capability of the underflow orifice is exceeded and particles begin to compete for the chance to escape in the underflow. This crowding effect can swamp the primary interaction — to the extent that the separation size can be estimated[6] from the mass recovery to the underflow.

Spherical particles

The effect of neighbouring particles on the fluid flow behaviour has been investigated by a number of workers,[7–10] the results being quoted in convenient summary form by Orr.[11] The actual velocity of a particle (u_p) in a suspension of concentration $\overline{C}_v$ can be related to the velocity (u_{p0}) that it would attain with $\overline{C}_v = 0$ by the equation

$$u_p = u_{p0}\,(1-\overline{C}_v)^{\beta} \qquad (25)$$

in which β is an exponent that varies with the Reynolds number for the relative motion between particle and fluid. A table of values for β was published by Orr,[11] but for laminar and near-laminar motion an average value of 4.4 should be acceptable.

Applying the correction to u_p and putting $E = 24$ in equation 20 gives

$$d_{50} = \sqrt{\frac{18\eta}{(\sigma-\rho)a}\cdot\frac{u_p}{(1-\overline{C}_v)^{4.4}}} \qquad (26)$$

and equation 26 has been tested against average data[4] quoted for spherical particles of specific gravity 2.6 at a concentration of 50 g/l or 4.85% w/w. The cyclone

Table 4 Average cyclone performance

Cyclone diameter, mm	Pressure drop, bar	Capacity, m³/h	Height to diameter ratios n_1+n_2	n_1	n_2	Separation size, μm, 50 g/l From	To
50	4	6.0	4	1.5	2.5	6.5	9.5
100	3	20.8	3.5	1.5	2	10.5	15.5
200	2	67.9	3	1.5	1.5	17.5	26.5
500	1	350	2.5	1	1.5	36	54
1250	0.5	1326	1.5	0.5	1	88	132

information (Table 4) did not include any subdivision of the total cyclone height into the cylindrical and conical components, so the values of n_1 and n_2 shown were assigned arbitrarily. The predicted separations are shown in Table 5 and the d_{50} sizes have been plotted in Fig. 3 together with the ranges from Table 2. The predicted d_{50} sizes all fall within the quoted ranges, even though the assumption of laminar motion is becoming somewhat strained with a Reynolds number of 24.7 for the 1250-mm diameter cyclone.

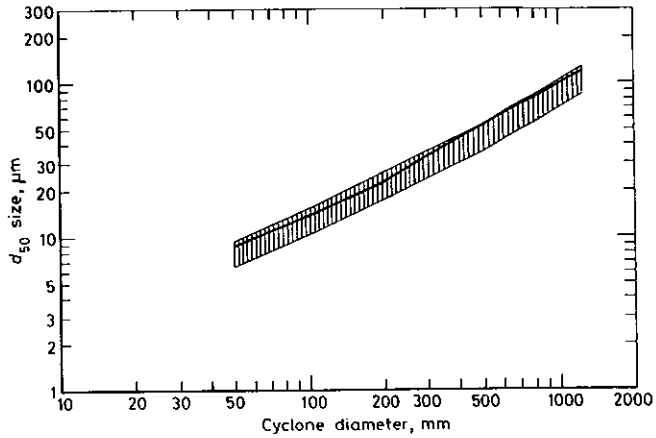

Fig. 3 d_{50} predictions (corrected for 4.85% solids)

Irregular shaped particles

The formidable difficulties associated with any analysis of the hydrodynamic behaviour of irregular shaped particles have led to the use of empirically based methods of correction. It is usual practice to assume that a relationship such as that given in equation 25 holds for irregular shapes, but with a considerable increase in the value of β.

If the data quoted in Table 2 are used as a guide, a concentration of 250 g/l ($\overline{C}_v = 0.09434$) doubles the separation size. Under laminar conditions the particle velocity is proportional to the square of the size, so the velocity ratio becomes

$$\frac{u_p}{u_{p0}} = \frac{1}{2^2} = (1-0.09434)^{\beta}$$

and

$$\beta = \frac{\ln 1/4}{\ln (0.9057)} = 14.0$$

Thus, for irregular shaped particles equation 24 becomes

$$d_{50} = \sqrt{18\left(1+\frac{6}{2^{10k}}\right)\frac{\eta}{(\sigma-\rho)a}\cdot\frac{u_p}{(1-\overline{C}_v)^{14}}} \qquad (27)$$

The d_{50} sizes predicted by equation 27 have been plotted in Fig. 4 together with the ranges quoted in Table 2 for 250 g/l of solids (21.63% w/w) and, on comparison with Fig. 2, the consistency of the correction factor is evident.

Conclusion

The separation model presented in this paper is based on simple bulk flow considerations and omits many of the

Table 5 Predicted separation ($\sigma = 2.6$, $k = \pi/6$)

Cyclone diameter, mm	Tangential velocity, cm/s	Radial acceleration, g	Total angle, rad	Radial velocity, cm/s	Laminar d_{50}, μm	Reynolds number
50	2828	3263	155	20.3	8.8	1.79
100	2450	1224	144	19.1	14.0	2.67
200	2000	408	133	17.1	22.9	3.91
500	1414	81.6	85.7	18.5	53.2	9.85
1250	1000	16.3	55.5	20.0	123.7	24.7

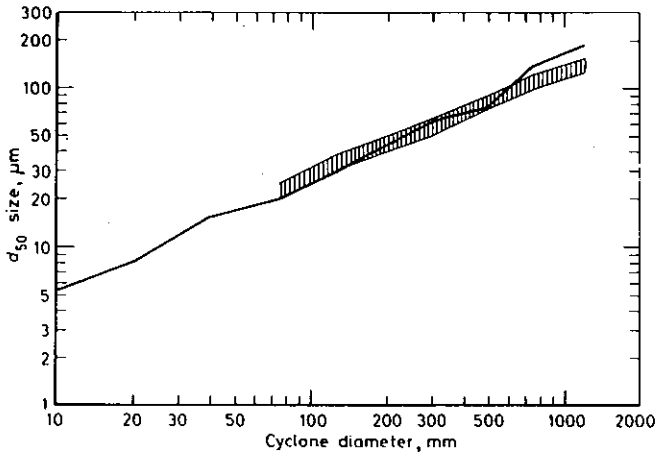

Fig. 4 d_{50} predictions (corrected for 21.63% solids)

variables that are commonly included in hydrocyclone studies, such as the diameters of overflow and underflow orifices and the depth of the vortex finder. A more fundamental difference is that the average forces and flow effects are evaluated with reference to the cyclone diameter rather than to some internal separation surface, which greatly simplifies the calculations. The most radical feature, however, is that the particle radial velocities are calculated from the depletion in the solids concentration of the bulk flow, and the opposing fluid flow to the axis is included as an additive velocity component rather than as the prime mechanism in determining the cut size.

Any time-average model usually contains some compensatory effects, and in the present case the omission of the overflow and underflow orifices as variables will be compensated to some extent by specification of the pressure drop and volumetric capacity of the hydrocyclone as input variables. Similar effects probably occur in relation to the use of the maximum possible average inlet velocity in conjunction with the cyclone diameter rather than some lower velocity operative at a smaller radius of motion.

The simplicity of the model is achieved by basing it on optimal separation conditions and it cannot be applied under extreme conditions – for example, at abnormally high feed densities, or with unusual feed size distributions, or with pronounced throttling of the underflow orifice. These restrictions, however, leave a considerable range of conditions for which the proposed model may prove useful.

References

1. Fahlstrom P. H. Some aspects of the application of hydraulic cyclones in low grade ore milling. *OEEC Mission – Sweden* no. 127, 1953.
2. Holland-Batt A. B. A quantitative model of the motion of particles in the RSM/Mintek on-stream particle size analyser. *Powder Technol.*, 11, 1975, 11–25.
3. Heywood H. Uniform and non-uniform motion of particles in fluids. In *Proceedings of the symposium on the interaction of fluids and particles, London, 1962* (London: Institution of Chemical Engineers, 1962), 1–8.
4. Trawinski H. Hydrocyclones. In *Solid/liquid separation equipment scale-up* Purchas D. ed. (Croydon, England: Uplands Press, Ltd., 1977), 241–87.
5. Amberger Kaolinwerke GmbH. *Fachwörter Englisch–Deutsch und Formeln der Hydrozyklon-Praxis* (Amberg: the Company, n.d.), 20 p.
6. Fahlstrom P. H. Studies of the hydrocyclone as a classifier. In *Mineral processing* Roberts A. ed. (Oxford, etc.: Pergamon, 1965), 87–114. (*Proc. 6th Int. Mineral Process. Congr., Cannes, 1963*)
7. Steinour H. H. Rate of sedimentation. *Ind. Engng Chem.*, 36, 1944, 618–24.
8. Richardson J. F. and Zaki W. N. The sedimentation of a suspension of uniform spheres under conditions of viscous flow. *Chem. Engng Sci.*, 3, 1954, 65–73.
9. Burgers J. M. Influence of the concentration of a suspension on the sedimentation velocity. *Proc. Acad. Sci. Amsterdam*, 45, 1942, 9–16; 126–7.
10. Maude A. D. and Whitmore R. L. A generalised theory of sedimentation. *Brit. J. appl. Phys.*, 9, 1958, 477–81.
11. Orr C. *Particulate technology* (London: Macmillan, 1966), 7, 301.

Symbols

a	Acceleration, cm/s^2
A_c	Wall area of cyclone parallel to central axis, cm^2
A_x	Cross-sectional area of particle, cm^2
C	Drag coefficient for particle-fluid motion
C_T	Drag coefficient at terminal velocity, u_T
C_v	Volume concentration of particles of size d within cyclone
C_{v0}	Volume concentration of particles of size d in feed
$\overline{C}_v$	Average volume concentration of solids in feed
d	Particle size (projected area diameter), cm
d_{50}	Particle size reporting 50% by weight to overflow, underflow, cm
D	Diameter of cylindrical section of hydrocyclone, cm
E	Constant in drag coefficient equation
E_r	Volume flux of particles in radial direction
E_α	Volume flux of particles in tangential direction
g	Acceleration due to gravity, cm/s^2
h	Fluid head equivalent to pressure drop, p, m
k	Volume coefficient for particles
n_1	Cylinder height ÷ cyclone diameter
n_2	Cone height ÷ cyclone diameter
p	Pressure drop across cyclone, bar
Q	Volumetric feedrate to cyclone, m^3/h
r	Radius of motion, cm
R	Reynolds number at velocity u
R_T	Reynolds number at terminal velocity u_T
t	Mean retention time in cyclone, s
u	Particle radial velocity relative to cyclone wall, cm/s
u_p	Particle radial velocity relative to fluid at concentration $\overline{C}_v$, cm/s
u_{p0}	Particle radial velocity relative to fluid at concentration $\overline{C}_v = 0$, cm/s
u_T	Terminal velocity of particle relative to fluid, cm/s
U	Fluid radial velocity, cm/s
V_p	Volume of particle of size d, cm^3
V_c	Internal volume of hydrocyclone, cm^3
α	Extent of angular motion, rad
β	Exponent in concentration equation
v	Particle tangential velocity, cm/s
σ	Particle specific gravity
ρ	Fluid specific gravity
η	Fluid viscosity, P

Oxidation of zinc vapour by hydrogen–water vapour–carbon dioxide–carbon monoxide–argon mixtures

J. A. Clarke B.Sc., Ph.D., D.M.S., M.I.M.M.
Johnson Matthey Chemicals, Ltd., Enfield, Middlesex, England (formerly Department of Metallurgy and Materials Science, University of Cambridge, England)

D. J. Fray M.A., B.Sc.(Eng.), A.R.S.M., Ph.D., D.I.C., M.I.M., M.I.M.M.
Department of Metallurgy and Materials Science, University of Cambridge, England

542.943:546.47.001.4

Synopsis
The oxidation of zinc vapour in H_2–H_2O–CO–CO_2–A mixtures has been studied over the temperature range 973–1173K. The reaction occurred entirely on the walls of the silica tube and the rate was very much smaller than that calculated on the assumption of diffusion control. It was found that the rate was intermediate between the CO–CO_2 and the H_2–H_2O systems and that two regions could be distinguished. The morphology of the deposit was examined with the aid of the scanning electron microscope and the results were related to the deposits found in the Imperial Smelting Furnace.

The gases that issue from the Imperial Smelting Furnace consist mainly of $Zn_{(v)}$, CO, CO_2 and N_2, together with a small amount of hydrogen and water vapour.[1,2] To condense the zinc with minimum oxidation the zinc vapour is absorbed in a shower of molten lead droplets. Plant experience and laboratory studies[3,4,5] have shown that the reoxidation reaction takes place predominantly on solid surfaces, such as the walls of the crossovers and condensers, and on entrained particles of dust, sulphide and fume in the gas stream, but, with present operating techniques, approximately 95% of the zinc vapour that enters the condenser is absorbed, the remainder collecting as a dross and as blue powder scrubbed from the exhaust gases. This leads to the conclusion that the kinetics of zinc absorption into the lead droplets must be much faster than the kinetics of oxidation.

Previous work has concentrated on the oxidation in CO–CO_2[3,4] and H_2–H_2O[5] mixtures and it has been shown that the reaction rate for the H_2O oxidation is considerably faster than that for CO_2 oxidation. Plant studies have indicated, however, that the presence of small quantities of water vapour (1.5–2.0%) has little effect on furnace performance and, therefore, the reaction rate noted above may not be applicable under furnace conditions. Any water that is in the furnace enters with the air blast or through accidental leaks, but the quantities of water usually present in the furnace gas are too small to pose a major problem.

Manuscript first received by the Institution of Mining and Metallurgy on 17 December, 1981; revised manuscript received on 15 February, 1982. Paper published in *Trans. Instn Min. Metall. (Sect. C: Mineral Process. Extr. Metall.)*, 91, March 1982.

Furnace operators are searching, however, for an alternative source of fuel, yet hydrocarbons, which are attractive from a calorific aspect, suffer from the disadvantage that copious quantities of water vapour are produced on combustion. Before these fuels are used in an Imperial Smelting Furnace (ISF), it is essential to know how much faster the zinc reoxidation reaction is in gas mixtures that contain H_2–H_2O–CO–CO_2–N_2. Unfortunately, it is not possible to calculate the rate of oxidation in this complex gas mixture because of interactions of the gases and, perhaps, adsorbed species. For this reason, it was decided to investigate the oxidation of $Zn_{(v)}$ in CO–CO_2–H_2–H_2O–A mixtures. This will indicate how increasing levels of water contents in the furnace gases will affect the efficiency of the condensation process. In addition, comparison of the deposits with those actually found in the furnace will give an indication of the relationship of this work to the conditions in an operating furnace.

Experimental procedure

The apparatus and technique were identical to those used in the previous studies.[4,5]

The deposits were examined under the scanning electron microscope. Material sampled from various positions in the Imperial Smelting blast-furnace gas offtake system was supplied by Imperial Smelting Processes, Ltd., Avonmouth, for a comparison with laboratory samples. As with those, no surface preparation was required, and the samples were rendered conductive merely by painting a Silverdag bridge between the specimen stub and the deposit. To complement the morphological examination, the surfaces were analysed with the aid of the Edax attachment to the scanning microscope.

Results

The results obtained are given in Tables 1–4. Typical morphology of the deposits is shown in Fig. 1, and Figs. 2–4 show the morphologies of the samples from the blast-furnace. Fig. 7 shows the morphology of zinc deposits found at the cooler end of the tube.

Discussion of results

In the previous studies it was necessary to consider only the individual reactions

$$Zn_{(v)} + CO_2 \rightarrow ZnO + CO \quad (1)$$

$$Zn_{(v)} + H_2O \rightarrow ZnO + H_2 \quad (2)$$

whereas, in this work, it is essential to take account of the simultaneous occurrence of these reactions and the reaction

$$CO_2 + H_2 \rightarrow H_2O + CO \quad (3)$$

It was found that fast reaction rates were often encountered and equilibrium conditions approached. As the gas composition changed along the tube, the reaction rate altered and two regions were observed (Fig. 5): this indicates a linear relationship between the reaction rate and the zinc partial pressure with a change of slope at p_{Zn} of 0.05 atm. At very low flow rates the higher rate region was often missed, as the reaction was completed at the very start of the constant temperature zone of the reactor tube. A higher flow rate increased the extent to which this region was observable, but did not change the slope of the plots.

The main unknown in this work is the extent to which reaction 3 proceeds. This reaction has been studied